

Measurement of $|V_{cb}|$ and the Form-Factor Slope in $\bar{B} \rightarrow D\ell^-\bar{\nu}_\ell$ Decays in Events Tagged by a Fully Reconstructed B Meson

B. Aubert,¹ Y. Karyotakis,¹ J. P. Lees,¹ V. Poireau,¹ E. Prencipe,¹ X. Prudent,¹ V. Tisserand,¹ J. Garra Tico,² E. Grauges,² M. Martinelli^{ab,3} A. Palano^{ab,3} M. Pappagallo^{ab,3} G. Eigen,⁴ B. Stugu,⁴ L. Sun,⁴ M. Battaglia,⁵ D. N. Brown,⁵ L. T. Kerth,⁵ Yu. G. Kolomensky,⁵ G. Lynch,⁵ I. L. Osipenkov,⁵ K. Tackmann,⁵ T. Tanabe,⁵ C. M. Hawkes,⁶ N. Soni,⁶ A. T. Watson,⁶ H. Koch,⁷ T. Schroeder,⁷ D. J. Asgeirsson,⁸ B. G. Fulsom,⁸ C. Hearty,⁸ T. S. Mattison,⁸ J. A. McKenna,⁸ M. Barrett,⁹ A. Khan,⁹ A. Randle-Conde,⁹ V. E. Blinov,¹⁰ A. D. Bukin,^{10,*} A. R. Buzykaev,¹⁰ V. P. Druzhinin,¹⁰ V. B. Golubev,¹⁰ A. P. Onuchin,¹⁰ S. I. Serednyakov,¹⁰ Yu. I. Skovpen,¹⁰ E. P. Solodov,¹⁰ K. Yu. Todyshev,¹⁰ M. Bondioli,¹¹ S. Curry,¹¹ I. Eschrich,¹¹ D. Kirkby,¹¹ A. J. Lankford,¹¹ P. Lund,¹¹ M. Mandelkern,¹¹ E. C. Martin,¹¹ D. P. Stoker,¹¹ H. Atmacan,¹² J. W. Gary,¹² F. Liu,¹² O. Long,¹² G. M. Vitug,¹² Z. Yasin,¹² L. Zhang,¹² V. Sharma,¹³ C. Campagnari,¹⁴ T. M. Hong,¹⁴ D. Kovalskyi,¹⁴ M. A. Mazur,¹⁴ J. D. Richman,¹⁴ T. W. Beck,¹⁵ A. M. Eisner,¹⁵ C. A. Heusch,¹⁵ J. Kroseberg,¹⁵ W. S. Lockman,¹⁵ A. J. Martinez,¹⁵ T. Schalk,¹⁵ B. A. Schumm,¹⁵ A. Seiden,¹⁵ L. Wang,¹⁵ L. O. Winstrom,¹⁵ C. H. Cheng,¹⁶ D. A. Doll,¹⁶ B. Echenard,¹⁶ F. Fang,¹⁶ D. G. Hitlin,¹⁶ I. Narsky,¹⁶ T. Piatenko,¹⁶ F. C. Porter,¹⁶ R. Andreassen,¹⁷ G. Mancinelli,¹⁷ B. T. Meadows,¹⁷ K. Mishra,¹⁷ M. D. Sokoloff,¹⁷ P. C. Bloom,¹⁸ W. T. Ford,¹⁸ A. Gaz,¹⁸ J. F. Hirschauer,¹⁸ M. Nagel,¹⁸ U. Nauenberg,¹⁸ J. G. Smith,¹⁸ S. R. Wagner,¹⁸ R. Ayad,^{19,†} W. H. Toki,¹⁹ R. J. Wilson,¹⁹ E. Feltresi,²⁰ A. Hauke,²⁰ H. Jasper,²⁰ T. M. Karbach,²⁰ J. Merkel,²⁰ A. Petzold,²⁰ B. Spaan,²⁰ K. Wacker,²⁰ M. J. Kobel,²¹ R. Nogowski,²¹ K. R. Schubert,²¹ R. Schwierz,²¹ A. Volk,²¹ D. Bernard,²² E. Latour,²² M. Verderi,²² P. J. Clark,²³ S. Playfer,²³ J. E. Watson,²³ M. Andreotti^{ab,24} D. Bettoni^{a,24} C. Bozzi^{a,24} R. Calabrese^{ab,24} A. Cecchi^{ab,24} G. Cibinetto^{ab,24} E. Fioravanti^{ab,24} P. Franchini^{ab,24} E. Luppi^{ab,24} M. Munerato^{ab,24} M. Negrini^{ab,24} A. Petrella^{ab,24} L. Piemontese^{a,24} V. Santoro^{ab,24} R. Baldini-Ferrolì,²⁵ A. Calcaterra,²⁵ R. de Sangro,²⁵ G. Finocchiaro,²⁵ S. Pacetti,²⁵ P. Patteri,²⁵ I. M. Peruzzi,^{25,‡} M. Piccolo,²⁵ M. Rama,²⁵ A. Zallo,²⁵ R. Contri^{ab,26} E. Guido,²⁶ M. Lo Vetere^{ab,26} M. R. Monge^{ab,26} S. Passaggio^{a,26} C. Patrignani^{ab,26} E. Robutti^{a,26} S. Tosi^{ab,26} K. S. Chaisanguanthum,²⁷ M. Morii,²⁷ A. Adametz,²⁸ J. Marks,²⁸ S. Schenk,²⁸ U. Uwer,²⁸ F. U. Bernlochner,²⁹ V. Klose,²⁹ H. M. Lacker,²⁹ D. J. Bard,³⁰ P. D. Dauncey,³⁰ M. Tibbetts,³⁰ P. K. Behera,³¹ M. J. Charles,³¹ U. Mallik,³¹ J. Cochran,³² H. B. Crawley,³² L. Dong,³² V. Eyges,³² W. T. Meyer,³² S. Prell,³² E. I. Rosenberg,³² A. E. Rubin,³² Y. Y. Gao,³³ A. V. Gritsan,³³ Z. J. Guo,³³ N. Arnaud,³⁴ J. Béquilleux,³⁴ A. D’Orazio,³⁴ M. Davier,³⁴ D. Derkach,³⁴ J. Firmino da Costa,³⁴ G. Grosdidier,³⁴ F. Le Diberder,³⁴ V. Lepeltier,³⁴ A. M. Lutz,³⁴ B. Malaescu,³⁴ S. Pruvot,³⁴ P. Roudeau,³⁴ M. H. Schune,³⁴ J. Serrano,³⁴ V. Sordini,^{34,§} A. Stocchi,³⁴ G. Wormser,³⁴ D. J. Lange,³⁵ D. M. Wright,³⁵ I. Bingham,³⁶ J. P. Burke,³⁶ C. A. Chavez,³⁶ J. R. Fry,³⁶ E. Gabathuler,³⁶ R. Gamet,³⁶ D. E. Hutchcroft,³⁶ D. J. Payne,³⁶ C. Touramanis,³⁶ A. J. Bevan,³⁷ C. K. Clarke,³⁷ F. Di Lodovico,³⁷ R. Sacco,³⁷ M. Sigamani,³⁷ G. Cowan,³⁸ S. Paramesvaran,³⁸ A. C. Wren,³⁸ D. N. Brown,³⁹ C. L. Davis,³⁹ A. G. Denig,⁴⁰ M. Fritsch,⁴⁰ W. Gradl,⁴⁰ A. Hafner,⁴⁰ K. E. Alwyn,⁴¹ D. Bailey,⁴¹ R. J. Barlow,⁴¹ G. Jackson,⁴¹ G. D. Lafferty,⁴¹ T. J. West,⁴¹ J. I. Yi,⁴¹ J. Anderson,⁴² C. Chen,⁴² A. Jawahery,⁴² D. A. Roberts,⁴² G. Simi,⁴² J. M. Tuggle,⁴² C. Dallapiccola,⁴³ E. Salvati,⁴³ S. Saremi,⁴³ R. Cowan,⁴⁴ D. Dujmic,⁴⁴ P. H. Fisher,⁴⁴ S. W. Henderson,⁴⁴ G. Sciolla,⁴⁴ M. Spitznagel,⁴⁴ R. K. Yamamoto,⁴⁴ M. Zhao,⁴⁴ P. M. Patel,⁴⁵ S. H. Robertson,⁴⁵ M. Schram,⁴⁵ A. Lazzaro^{ab,46} V. Lombardo^{a,46} F. Palombo^{ab,46} S. Stracka^{ab,46} J. M. Bauer,⁴⁷ L. Cremaldi,⁴⁷ R. Godang,^{47,¶} R. Kroeger,⁴⁷ P. Sonnek,⁴⁷ D. J. Summers,⁴⁷ H. W. Zhao,⁴⁷ M. Simard,⁴⁸ P. Taras,⁴⁸ H. Nicholson,⁴⁹ G. De Nardo^{ab,50} L. Lista^{a,50} D. Monorchio^{ab,50} G. Onorato^{ab,50} C. Sciacca^{ab,50} G. Raven,⁵¹ H. L. Snoek,⁵¹ C. P. Jessop,⁵² K. J. Knoepfel,⁵² J. M. LoSecco,⁵² W. F. Wang,⁵² L. A. Corwin,⁵³ K. Honscheid,⁵³ H. Kagan,⁵³ R. Kass,⁵³ J. P. Morris,⁵³ A. M. Rahimi,⁵³ J. J. Regensburger,⁵³ S. J. Sekula,⁵³ Q. K. Wong,⁵³ N. L. Blount,⁵⁴ J. Brau,⁵⁴ R. Frey,⁵⁴ O. Igonkina,⁵⁴ J. A. Kolb,⁵⁴ M. Lu,⁵⁴ R. Rahmat,⁵⁴ N. B. Sinev,⁵⁴ D. Strom,⁵⁴ J. Strube,⁵⁴ E. Torrence,⁵⁴ G. Castelli^{ab,55} N. Gagliardi^{ab,55} M. Margoni^{ab,55} M. Morandin^{a,55} M. Posocco^{a,55} M. Rotondo^{a,55} F. Simonetto^{ab,55} R. Stroili^{ab,55} C. Voci^{ab,55} P. del Amo Sanchez,⁵⁶ E. Ben-Haim,⁵⁶ G. R. Bonneaud,⁵⁶ H. Briand,⁵⁶ J. Chauveau,⁵⁶ O. Hamon,⁵⁶ Ph. Leruste,⁵⁶ G. Marchiori,⁵⁶ J. Ocariz,⁵⁶ A. Perez,⁵⁶ J. Prendki,⁵⁶ S. Sitt,⁵⁶ L. Gladney,⁵⁷ M. Biasini^{ab,58} E. Manoni^{ab,58} C. Angelini^{ab,59} G. Batignani^{ab,59}

S. Bettarini^{ab, 59} G. Calderini^{ab, 59, **} M. Carpinelli^{ab, 59, ††} A. Cervelli^{ab, 59} F. Forti^{ab, 59} M. A. Giorgi^{ab, 59}
 A. Lusiani^{ac, 59} M. Morganti^{ab, 59} N. Neri^{ab, 59} E. Paoloni^{ab, 59} G. Rizzo^{ab, 59} J. J. Walsh^{a, 59} D. Lopes Pegna,⁶⁰
 C. Lu,⁶⁰ J. Olsen,⁶⁰ A. J. S. Smith,⁶⁰ A. V. Telnov,⁶⁰ F. Anulli^{a, 61} E. Baracchini^{ab, 61} G. Cavoto^{a, 61} R. Faccini^{ab, 61}
 F. Ferrarotto^{a, 61} F. Ferroni^{ab, 61} M. Gaspero^{ab, 61} P. D. Jackson^{a, 61} L. Li Gioi^{a, 61} M. A. Mazzoni^{a, 61} S. Morganti^{a, 61}
 G. Piredda^{a, 61} F. Renga^{ab, 61} C. Voena^{a, 61} M. Ebert,⁶² T. Hartmann,⁶² H. Schröder,⁶² R. Waldi,⁶² T. Adye,⁶³
 B. Franek,⁶³ E. O. Olaiya,⁶³ F. F. Wilson,⁶³ S. Emery,⁶⁴ L. Esteve,⁶⁴ G. Hamel de Monchenault,⁶⁴ W. Kozanecki,⁶⁴
 G. Vasseur,⁶⁴ Ch. Yèche,⁶⁴ M. Zito,⁶⁴ M. T. Allen,⁶⁵ D. Aston,⁶⁵ R. Bartoldus,⁶⁵ J. F. Benitez,⁶⁵ R. Cenci,⁶⁵
 J. P. Coleman,⁶⁵ M. R. Convery,⁶⁵ J. C. Dingfelder,⁶⁵ J. Dorfan,⁶⁵ G. P. Dubois-Felsmann,⁶⁵ W. Dunwoodie,⁶⁵
 R. C. Field,⁶⁵ M. Franco Sevilla,⁶⁵ A. M. Gabareen,⁶⁵ M. T. Graham,⁶⁵ P. Grenier,⁶⁵ C. Hast,⁶⁵ W. R. Innes,⁶⁵
 J. Kaminski,⁶⁵ M. H. Kelsey,⁶⁵ H. Kim,⁶⁵ P. Kim,⁶⁵ M. L. Kocian,⁶⁵ D. W. G. S. Leith,⁶⁵ S. Li,⁶⁵ B. Lindquist,⁶⁵
 S. Luitz,⁶⁵ V. Luth,⁶⁵ H. L. Lynch,⁶⁵ D. B. MacFarlane,⁶⁵ H. Marsiske,⁶⁵ R. Messner,^{65, *} D. R. Muller,⁶⁵
 H. Neal,⁶⁵ S. Nelson,⁶⁵ C. P. O'Grady,⁶⁵ I. Ofte,⁶⁵ M. Perl,⁶⁵ B. N. Ratcliff,⁶⁵ A. Roodman,⁶⁵ A. A. Salnikov,⁶⁵
 R. H. Schindler,⁶⁵ J. Schwiening,⁶⁵ A. Snyder,⁶⁵ D. Su,⁶⁵ M. K. Sullivan,⁶⁵ K. Suzuki,⁶⁵ S. K. Swain,⁶⁵
 J. M. Thompson,⁶⁵ J. Va'vra,⁶⁵ A. P. Wagner,⁶⁵ M. Weaver,⁶⁵ C. A. West,⁶⁵ W. J. Wisniewski,⁶⁵ M. Wittgen,⁶⁵
 D. H. Wright,⁶⁵ H. W. Wulsin,⁶⁵ A. K. Yarritu,⁶⁵ C. C. Young,⁶⁵ V. Ziegler,⁶⁵ X. R. Chen,⁶⁶ H. Liu,⁶⁶ W. Park,⁶⁶
 M. V. Purohit,⁶⁶ R. M. White,⁶⁶ J. R. Wilson,⁶⁶ P. R. Burchat,⁶⁷ A. J. Edwards,⁶⁷ T. S. Miyashita,⁶⁷ S. Ahmed,⁶⁸
 M. S. Alam,⁶⁸ J. A. Ernst,⁶⁸ B. Pan,⁶⁸ M. A. Saeed,⁶⁸ S. B. Zain,⁶⁸ A. Soffer,⁶⁹ S. M. Spanier,⁷⁰ B. J. Wogslund,⁷⁰
 R. Eckmann,⁷¹ J. L. Ritchie,⁷¹ A. M. Ruland,⁷¹ C. J. Schilling,⁷¹ R. F. Schwitters,⁷¹ B. C. Wray,⁷¹
 B. W. Drummond,⁷² J. M. Izen,⁷² X. C. Lou,⁷² F. Bianchi^{ab, 73} D. Gamba^{ab, 73} M. Pelliccioni^{ab, 73} M. Bomben^{ab, 74}
 L. Bosisio^{ab, 74} C. Cartaro^{ab, 74} G. Della Ricca^{ab, 74} L. Lanceri^{ab, 74} L. Vitale^{ab, 74} V. Azzolini,⁷⁵ N. Lopez-March,⁷⁵
 F. Martinez-Vidal,⁷⁵ D. A. Milanes,⁷⁵ A. Oyanguren,⁷⁵ J. Albert,⁷⁶ Sw. Banerjee,⁷⁶ B. Bhuyan,⁷⁶ H. H. F. Choi,⁷⁶
 K. Hamano,⁷⁶ G. J. King,⁷⁶ R. Kowalewski,⁷⁶ M. J. Lewczuk,⁷⁶ I. M. Nugent,⁷⁶ J. M. Roney,⁷⁶ R. J. Sobie,⁷⁶
 T. J. Gershon,⁷⁷ P. F. Harrison,⁷⁷ J. Ilic,⁷⁷ T. E. Latham,⁷⁷ G. B. Mohanty,⁷⁷ E. M. T. Puccio,⁷⁷
 H. R. Band,⁷⁸ X. Chen,⁷⁸ S. Dasu,⁷⁸ K. T. Flood,⁷⁸ Y. Pan,⁷⁸ R. Prepost,⁷⁸ C. O. Vuosalo,⁷⁸ and S. L. Wu⁷⁸

(The BABAR Collaboration)

¹Laboratoire d'Annecy-le-Vieux de Physique des Particules (LAPP),

Université de Savoie, CNRS/IN2P3, F-74941 Annecy-Le-Vieux, France

²Universitat de Barcelona, Facultat de Física, Departament ECM, E-08028 Barcelona, Spain

³INFN Sezione di Bari^a; Dipartimento di Fisica, Università di Bari^b, I-70126 Bari, Italy

⁴University of Bergen, Institute of Physics, N-5007 Bergen, Norway

⁵Lawrence Berkeley National Laboratory and University of California, Berkeley, California 94720, USA

⁶University of Birmingham, Birmingham, B15 2TT, United Kingdom

⁷Ruhr Universität Bochum, Institut für Experimentalphysik 1, D-44780 Bochum, Germany

⁸University of British Columbia, Vancouver, British Columbia, Canada V6T 1Z1

⁹Brunel University, Uxbridge, Middlesex UB8 3PH, United Kingdom

¹⁰Budker Institute of Nuclear Physics, Novosibirsk 630090, Russia

¹¹University of California at Irvine, Irvine, California 92697, USA

¹²University of California at Riverside, Riverside, California 92521, USA

¹³University of California at San Diego, La Jolla, California 92093, USA

¹⁴University of California at Santa Barbara, Santa Barbara, California 93106, USA

¹⁵University of California at Santa Cruz, Institute for Particle Physics, Santa Cruz, California 95064, USA

¹⁶California Institute of Technology, Pasadena, California 91125, USA

¹⁷University of Cincinnati, Cincinnati, Ohio 45221, USA

¹⁸University of Colorado, Boulder, Colorado 80309, USA

¹⁹Colorado State University, Fort Collins, Colorado 80523, USA

²⁰Technische Universität Dortmund, Fakultät Physik, D-44221 Dortmund, Germany

²¹Technische Universität Dresden, Institut für Kern- und Teilchenphysik, D-01062 Dresden, Germany

²²Laboratoire Leprince-Ringuet, CNRS/IN2P3, Ecole Polytechnique, F-91128 Palaiseau, France

²³University of Edinburgh, Edinburgh EH9 3JZ, United Kingdom

²⁴INFN Sezione di Ferrara^a; Dipartimento di Fisica, Università di Ferrara^b, I-44100 Ferrara, Italy

²⁵INFN Laboratori Nazionali di Frascati, I-00044 Frascati, Italy

²⁶INFN Sezione di Genova^a; Dipartimento di Fisica, Università di Genova^b, I-16146 Genova, Italy

²⁷Harvard University, Cambridge, Massachusetts 02138, USA

²⁸Universität Heidelberg, Physikalisches Institut, Philosophenweg 12, D-69120 Heidelberg, Germany

²⁹Humboldt-Universität zu Berlin, Institut für Physik, Newtonstr. 15, D-12489 Berlin, Germany

³⁰Imperial College London, London, SW7 2AZ, United Kingdom

³¹University of Iowa, Iowa City, Iowa 52242, USA

- ³²Iowa State University, Ames, Iowa 50011-3160, USA
- ³³Johns Hopkins University, Baltimore, Maryland 21218, USA
- ³⁴Laboratoire de l'Accélérateur Linéaire, IN2P3/CNRS et Université Paris-Sud 11, Centre Scientifique d'Orsay, B. P. 34, F-91898 Orsay Cedex, France
- ³⁵Lawrence Livermore National Laboratory, Livermore, California 94550, USA
- ³⁶University of Liverpool, Liverpool L69 7ZE, United Kingdom
- ³⁷Queen Mary, University of London, London, E1 4NS, United Kingdom
- ³⁸University of London, Royal Holloway and Bedford New College, Egham, Surrey TW20 0EX, United Kingdom
- ³⁹University of Louisville, Louisville, Kentucky 40292, USA
- ⁴⁰Johannes Gutenberg-Universität Mainz, Institut für Kernphysik, D-55099 Mainz, Germany
- ⁴¹University of Manchester, Manchester M13 9PL, United Kingdom
- ⁴²University of Maryland, College Park, Maryland 20742, USA
- ⁴³University of Massachusetts, Amherst, Massachusetts 01003, USA
- ⁴⁴Massachusetts Institute of Technology, Laboratory for Nuclear Science, Cambridge, Massachusetts 02139, USA
- ⁴⁵McGill University, Montréal, Québec, Canada H3A 2T8
- ⁴⁶INFN Sezione di Milano^a; Dipartimento di Fisica, Università di Milano^b, I-20133 Milano, Italy
- ⁴⁷University of Mississippi, University, Mississippi 38677, USA
- ⁴⁸Université de Montréal, Physique des Particules, Montréal, Québec, Canada H3C 3J7
- ⁴⁹Mount Holyoke College, South Hadley, Massachusetts 01075, USA
- ⁵⁰INFN Sezione di Napoli^a; Dipartimento di Scienze Fisiche, Università di Napoli Federico II^b, I-80126 Napoli, Italy
- ⁵¹NIKHEF, National Institute for Nuclear Physics and High Energy Physics, NL-1009 DB Amsterdam, The Netherlands
- ⁵²University of Notre Dame, Notre Dame, Indiana 46556, USA
- ⁵³Ohio State University, Columbus, Ohio 43210, USA
- ⁵⁴University of Oregon, Eugene, Oregon 97403, USA
- ⁵⁵INFN Sezione di Padova^a; Dipartimento di Fisica, Università di Padova^b, I-35131 Padova, Italy
- ⁵⁶Laboratoire de Physique Nucléaire et de Hautes Energies, IN2P3/CNRS, Université Pierre et Marie Curie-Paris6, Université Denis Diderot-Paris7, F-75252 Paris, France
- ⁵⁷University of Pennsylvania, Philadelphia, Pennsylvania 19104, USA
- ⁵⁸INFN Sezione di Perugia^a; Dipartimento di Fisica, Università di Perugia^b, I-06100 Perugia, Italy
- ⁵⁹INFN Sezione di Pisa^a; Dipartimento di Fisica, Università di Pisa^b; Scuola Normale Superiore di Pisa^c, I-56127 Pisa, Italy
- ⁶⁰Princeton University, Princeton, New Jersey 08544, USA
- ⁶¹INFN Sezione di Roma^a; Dipartimento di Fisica, Università di Roma La Sapienza^b, I-00185 Roma, Italy
- ⁶²Universität Rostock, D-18051 Rostock, Germany
- ⁶³Rutherford Appleton Laboratory, Chilton, Didcot, Oxon, OX11 0QX, United Kingdom
- ⁶⁴CEA, Irfu, SPP, Centre de Saclay, F-91191 Gif-sur-Yvette, France
- ⁶⁵SLAC National Accelerator Laboratory, Stanford, California 94309 USA
- ⁶⁶University of South Carolina, Columbia, South Carolina 29208, USA
- ⁶⁷Stanford University, Stanford, California 94305-4060, USA
- ⁶⁸State University of New York, Albany, New York 12222, USA
- ⁶⁹Tel Aviv University, School of Physics and Astronomy, Tel Aviv, 69978, Israel
- ⁷⁰University of Tennessee, Knoxville, Tennessee 37996, USA
- ⁷¹University of Texas at Austin, Austin, Texas 78712, USA
- ⁷²University of Texas at Dallas, Richardson, Texas 75083, USA
- ⁷³INFN Sezione di Torino^a; Dipartimento di Fisica Sperimentale, Università di Torino^b, I-10125 Torino, Italy
- ⁷⁴INFN Sezione di Trieste^a; Dipartimento di Fisica, Università di Trieste^b, I-34127 Trieste, Italy
- ⁷⁵IFIC, Universitat de Valencia-CSIC, E-46071 Valencia, Spain
- ⁷⁶University of Victoria, Victoria, British Columbia, Canada V8W 3P6
- ⁷⁷Department of Physics, University of Warwick, Coventry CV4 7AL, United Kingdom
- ⁷⁸University of Wisconsin, Madison, Wisconsin 53706, USA

(Dated: October 15, 2018)

We present a measurement of the Cabibbo-Kobayashi-Maskawa matrix element $|V_{cb}|$ and the form-factor slope ρ^2 in $\bar{B} \rightarrow D\ell^-\bar{\nu}_\ell$ decays based on 460 million $B\bar{B}$ events recorded at the $\Upsilon(4S)$ resonance with the BABAR detector. $\bar{B} \rightarrow D\ell^-\bar{\nu}_\ell$ decays are selected in events in which a hadronic decay of the second B meson is fully reconstructed. We measure the differential decay rate and determine $\mathcal{G}(1)|V_{cb}| = (43.0 \pm 1.9 \pm 1.4) \times 10^{-3}$ and $\rho^2 = 1.20 \pm 0.09 \pm 0.04$, where $\mathcal{G}(1)$ is the hadronic form factor at the point of zero recoil. We also determine the exclusive branching fractions and find $\mathcal{B}(B^- \rightarrow D^0\ell^-\bar{\nu}_\ell) = (2.31 \pm 0.08 \pm 0.09)\%$ and $\mathcal{B}(\bar{B}^0 \rightarrow D^+\ell^-\bar{\nu}_\ell) = (2.23 \pm 0.11 \pm 0.11)\%$.

PACS numbers: 13.20He,12.38.Qk,14.40Nd

In the Standard Model (SM) of electroweak interactions, the rate of the semileptonic $\bar{B} \rightarrow D\ell^-\bar{\nu}_\ell$ decay is proportional to the square of the Cabibbo-Kobayashi-Maskawa (CKM) [1] matrix element $|V_{cb}|$, which is a measure of the weak interaction coupling of the b to the c quark. The length of the side of the unitary triangle opposite to the well-measured angle β is proportional to the ratio $|V_{ub}/V_{cb}|$, making the determination of $|V_{cb}|$ important to test the SM description of CP symmetry violation. In addition, imprecise knowledge of $|V_{cb}|$ is an important uncertainty limiting comparison of measurements of CP violation in K meson decays with those in B meson decays [2].

Measurements of $|V_{cb}|$ have been performed in inclusive semileptonic B decays [3] and in the exclusive transitions $\bar{B} \rightarrow D\ell^-\bar{\nu}_\ell$ and $\bar{B} \rightarrow D^*\ell^-\bar{\nu}_\ell$ [4]. The most recent inclusive and exclusive determinations differ by more than two standard deviations, with the inclusive result more than twice as precise as the exclusive one [5]. Thus improvements in the measurements of exclusive decay rates are highly desirable, particularly for $\bar{B} \rightarrow D\ell^-\bar{\nu}_\ell$ decays, where the experimental uncertainties dominate. Measurements of $|V_{cb}|$ based on studies of $\bar{B} \rightarrow D\ell^-\bar{\nu}_\ell$ decays have previously been reported by the Belle [6], CLEO [7], ALEPH [8] and BABAR [4] Collaborations.

The $\bar{B} \rightarrow D\ell^-\bar{\nu}_\ell$ decay rate [9] is proportional to the square of the hadronic matrix element that describes the effects of strong interactions in $\bar{B} \rightarrow D$ transitions. In the limit of very small lepton masses ($\ell = e$ or μ), their effect can be parameterized by a single form factor $\mathcal{G}(w)$:

$$\frac{d\Gamma(\bar{B} \rightarrow D\ell\nu)}{dw} = \frac{G_F^2}{48\pi^3\hbar} M_D^3 (M_B + M_D)^2 (w^2 - 1)^{3/2} |V_{cb}|^2 \mathcal{G}^2(w), \quad (1)$$

where G_F is the Fermi coupling constant, and M_B and M_D are the masses of the B and D mesons, respectively. The variable w denotes the product of the B and D meson four-velocities V_B and V_D , $w = V_B \cdot V_D = (M_B^2 + M_D^2 - q^2)/(2M_B M_D)$, where $q^2 \equiv (p_B - p_D)^2$, and p_B and p_D are the four-momenta of the B and D mesons.

In the limit of infinite quark masses, $\mathcal{G}(w)$ coincides with the Isgur-Wise function [10]. This function is normalized to unity at zero recoil, where q^2 is maximum. Corrections to the heavy quark limit have been calculated based on unquenched [11] and quenched lattice QCD [12]. Thus $|V_{cb}|$ can be extracted by extrapolating the differential decay rate to $w = 1$. To reduce the uncertainties associated with this extrapolation, constraints on the shape of the form factor are necessary. Several functional forms have been proposed [13]. We adopt the parameterization suggested in Ref. [14], where the non-linear dependence

of the form factor on w is expressed in terms of a single shape parameter, the form-factor slope ρ^2 .

In this letter, we present a measurement of the differential decay rates for $\bar{B}^0 \rightarrow D^+\ell^-\bar{\nu}_\ell$ and $B^- \rightarrow D^0\ell^-\bar{\nu}_\ell$ decays. The analysis is based on data collected with the BABAR detector [15] at the PEP-II asymmetric-energy e^+e^- storage rings. The data consist of 417 fb^{-1} recorded at the $\Upsilon(4S)$ resonance, corresponding to approximately 460 million $B\bar{B}$ pairs. An additional sample of 40 fb^{-1} , collected at a center-of-mass (CM) energy 40 MeV below the $\Upsilon(4S)$ resonance, is used to study background from $e^+e^- \rightarrow f\bar{f}$ ($f = u, d, s, c, \tau$) continuum events. We also use samples of GEANT4 Monte Carlo (MC) simulated events that correspond to about three times the data sample size. The simulation models $\bar{B} \rightarrow D^{(*)}\ell^-\bar{\nu}_\ell$ decays using calculations based on Heavy Quark Effective Theory (HQET) [14], $\bar{B} \rightarrow D^{**}(\rightarrow D^{(*)}\pi)\ell^-\bar{\nu}_\ell$ decays using the ISGW2 model [16], and non-resonant $\bar{B} \rightarrow D^{(*)}\pi\ell^-\bar{\nu}_\ell$ decays using the Goity-Roberts model [17]. The MC simulation includes radiative effects such as bremsstrahlung in the detector material. QED final-state radiation is modeled by PHOTOS [18].

Semileptonic decays are selected in $B\bar{B}$ events in which a hadronic decay of the second B meson (B_{tag}) is fully reconstructed. This leads to a very clean sample of events and also provides a precise measurement of q^2 and hence w . We first reconstruct the semileptonic B decay, selecting a lepton with momentum in the CM frame p_ℓ^* larger than 0.6 GeV. For electrons, we search for a vertex formed in conjunction with a track of opposite charge and remove those with an invariant mass consistent with a photon conversion or a π^0 Dalitz decay. Candidate D^0 mesons that have the correct charge correlation with the lepton are reconstructed in the $K^-\pi^+$, $K^-\pi^+\pi^0$, $K^-\pi^+\pi^+\pi^-$, $K_S^0\pi^+\pi^-$, $K_S^0\pi^+\pi^-\pi^0$, $K_S^0\pi^0$, K^+K^- , $\pi^+\pi^-$, and $K_S^0K_S^0$ channels, and D^+ mesons in the $K^-\pi^+\pi^+$, $K^-\pi^+\pi^+\pi^0$, $K_S^0\pi^+$, $K_S^0\pi^+\pi^0$, $K^+K^-\pi^+$, $K_S^0K^+$, and $K_S^0\pi^+\pi^+\pi^-$ channels. $D^0(D^+)$ candidates are required to be within 2σ of the nominal $D^0(D^+)$ mass, where σ is approximately $8 \text{ MeV}/c^2$. In events with multiple $D\ell^-$ combinations, the candidate with the largest $D\ell^-$ vertex probability is selected. Events with more than one reconstructed lepton with $p_\ell^* > 0.6 \text{ GeV}$ are vetoed.

We reconstruct B_{tag} decays [19] in charmed hadronic modes $\bar{B} \rightarrow D^{(*)}Y$, where Y represents a collection of hadrons, composed of $n_1\pi^\pm + n_2K^\pm + n_3K_S^0 + n_4\pi^0$, where $n_1 + n_2 = 1, 3, 5$, $n_3 \leq 2$, and $n_4 \leq 2$. Using $D^0(D^+)$ and $D^{*0}(D^{*+})$ as seeds for $B^-(\bar{B}^0)$ decays, we reconstruct about 1000 different decay modes. The kinematic consistency of a B_{tag} candidate with a B meson decay is evaluated using two variables: the beam-energy substituted mass $m_{ES} \equiv \sqrt{s/4 - (p_B^*)^2}$, and the energy difference $\Delta E \equiv E_B^* - \sqrt{s}/2$. Here \sqrt{s} is the total CM energy, and p_B^* and E_B^* denote the momentum and energy of the B_{tag} candidate in the CM frame. For correctly

identified B_{tag} decays, m_{ES} peaks at the B -meson mass, while ΔE is consistent with zero. We select B_{tag} candidates in the signal region defined as $5.27 \text{ GeV} < m_{ES} < 5.29 \text{ GeV}$, excluding those that have daughters in common with the $\bar{B} \rightarrow D\ell^-\bar{\nu}_\ell$ decay. In the case of multiple B_{tag} candidates in an event, we select the one with the smallest $|\Delta E|$ value. The B_{tag} and the $D\ell^-$ candidates are required to have the correct charge-flavor correlation. Cross-feed events, *i.e.*, $B_{\text{tag}}^-(\bar{B}_{\text{tag}}^0)$ candidates erroneously reconstructed as a neutral (charged) B meson, are subtracted using estimates from the simulation.

Semileptonic B decays are identified by their missing-mass squared value, $m_{\text{miss}}^2 = [p(\Upsilon(4S)) - p(B_{\text{tag}}) - p(D) - p(\ell)]^2$, defined in terms of the measured particle four-momenta. For correctly reconstructed signal events, the only missing particle is the neutrino and m_{miss}^2 peaks at zero. Other semileptonic B decays, like $\bar{B} \rightarrow D^{(*,**)}\ell^-\bar{\nu}_\ell$, where at least one particle is not reconstructed (feed-down), yield larger values of m_{miss}^2 .

We measure $|V_{cb}|$ and the form-factor slope ρ^2 by a fit to the w distribution. We examine the data and MC events in ten equal-size w bins in the interval $1 < w < 1.6$. Since the B momentum is known from the fully reconstructed B_{tag} in the same event, w can be reconstructed with good precision, namely to ~ 0.01 , which corresponds to about 2% of the full kinematic range.

To obtain the $\bar{B} \rightarrow D\ell^-\bar{\nu}_\ell$ signal yield in each bin of w , we perform a one-dimensional extended binned maximum likelihood fit [20] to the corresponding m_{miss}^2 distribution. The fitted data samples are assumed to contain four different types of events: $\bar{B} \rightarrow D\ell^-\bar{\nu}_\ell$ signal events, feed-down from other semileptonic B decays, combinatorial $B\bar{B}$ and continuum background, and fake lepton events (mostly from hadronic B decays with hadrons misidentified as leptons). The Probability Density Functions (PDFs) are derived from the MC predictions for the different semileptonic B decay m_{miss}^2 distributions. We use the off-peak data to provide the continuum background normalization. The shape of the continuum background distribution predicted by the MC simulation is consistent with that obtained from the off-peak data.

The measured m_{miss}^2 distributions are compared with the results of the fits for two different w intervals in Fig. 1.

We perform a least-squares fit to the observed signal yields in the ten bins of w . We minimize a χ^2 defined as

$$\chi^2 = \sum_{i=1}^{10} \frac{(N_{\text{data}}^i - \sum_{j=1}^{N_{\text{MC}}} W_j^i)^2}{(\sigma_{\text{data}}^i)^2 + \sum_{j=1}^{N_{\text{MC}}} W_j^i{}^2}, \quad (2)$$

where the index i refers to the w bin and the index j runs over all MC events in bin i ; N_{data}^i is the observed number of signal events found in the i^{th} bin and σ_{data}^i the corresponding uncertainty. The expected signal yields are calculated at each step of the minimization from the

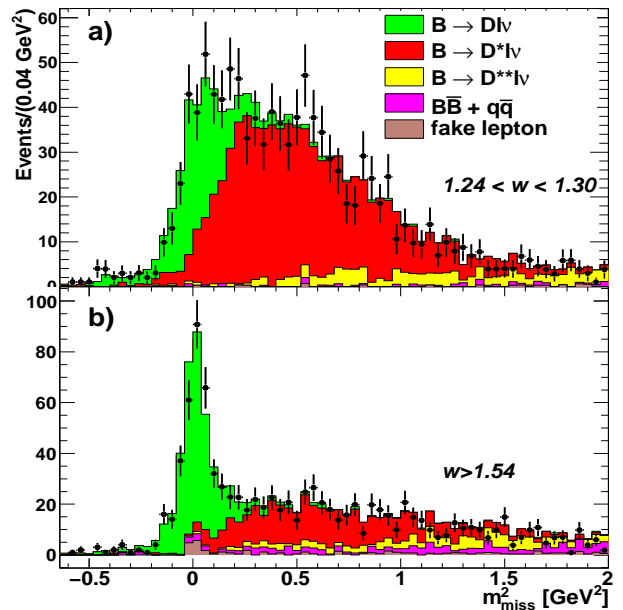


FIG. 1: (Color online) Fit to the m_{miss}^2 distribution, in two different w intervals, for $B^- \rightarrow D^0\ell^-\bar{\nu}_\ell$: the data (points with error bars) are compared to the results of the overall fit (sum of the solid histograms). The PDFs for the different fit components are stacked in the order shown in the legend.

reweighted sum of N_{MC}^i simulated events. Each weight is the product of two terms, $W_j^i = W^{\mathcal{L}} \times W_j^{i,\text{theo}}$ where $W^{\mathcal{L}}$ is an overall fixed scale factor, which accounts for the relative integrated luminosity of the data and signal MC events, and $W_j^{i,\text{theo}}$ is computed using the true w value of the event j and depends on $\mathcal{G}(1)|V_{cb}|$ and ρ^2 , which are free parameters determined in the fit that are recalculated at each step of the minimization.

We first fit the w distributions for the charged and neutral $\bar{B} \rightarrow D\ell^-\bar{\nu}_\ell$ samples separately, and then perform a fit to the combined $\bar{B} \rightarrow D\ell^-\bar{\nu}_\ell$ sample. In Fig. 2 we show the comparison between the data and the fit results for the combined sample. The measured values of $\mathcal{G}(1)|V_{cb}|$ and ρ^2 , with the corresponding correlation ρ_{corr} obtained from the fit, are reported in Table I. The value of the branching fraction is computed by integrating the differential expression in Eq. 1 and dividing by the appropriate B -meson lifetime.

In order to reduce the systematic uncertainty on the measurement of $\mathcal{G}(1)|V_{cb}|$ and the branching fractions, we normalize the exclusive signal yield to the yield of inclusive semileptonic decays, $\bar{B} \rightarrow X\ell^-\bar{\nu}_\ell$, in events tagged by a fully reconstructed hadronic B decay. The inclusive $\bar{B} \rightarrow X\ell^-\bar{\nu}_\ell$ decays are selected by identifying one charged lepton with $p_\ell^* > 0.6 \text{ GeV}$ and the charge expected based on the B_{tag} decay. In the case of multiple B_{tag} candidates in an event, we select the decay mode with the highest purity, estimated from the MC prediction for the fraction of true decays in the m_{ES} signal re-

TABLE I: Fit results for each sample. In the last column we report the results for the \bar{B}^0 and B^- combined fit, where the branching fraction refers to \bar{B}^0 decays. We also report the signal yields and the reconstruction efficiencies, integrated over the full w range. For $\mathcal{G}(1)|V_{cb}|$ and ρ^2 , we report both the statistical and systematic uncertainties.

	$B^- \rightarrow D^0 \ell^- \bar{\nu}_\ell$	$\bar{B}^0 \rightarrow D^+ \ell^- \bar{\nu}_\ell$	$B \rightarrow D \ell^- \bar{\nu}_\ell$
$\mathcal{G}(1) V_{cb} \cdot 10^3$	$41.7 \pm 2.1 \pm 1.3$	$45.6 \pm 3.3 \pm 1.6$	$43.0 \pm 1.9 \pm 1.4$
ρ^2	$1.14 \pm 0.11 \pm 0.04$	$1.29 \pm 0.14 \pm 0.05$	$1.20 \pm 0.09 \pm 0.04$
ρ_{corr}	0.943	0.950	0.952
χ^2/ndf	3.4/8	5.6/8	9.9/18
Signal Yield	2147 ± 69	1108 ± 45	-
Recon. efficiency	$(1.99 \pm 0.02) \times 10^{-4}$	$(1.09 \pm 0.02) \times 10^{-4}$	-
\mathcal{B}	$(2.31 \pm 0.08 \pm 0.09)\%$	$(2.23 \pm 0.11 \pm 0.11)\%$	$(2.17 \pm 0.06 \pm 0.09)\%$

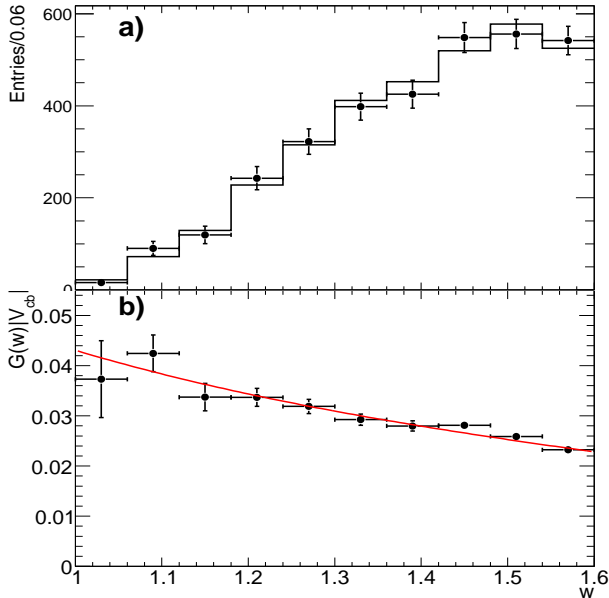


FIG. 2: (a) w distribution obtained summing $B^- \rightarrow D^0 \ell^- \bar{\nu}_\ell$ and $\bar{B}^0 \rightarrow D^+ \ell^- \bar{\nu}_\ell$ yields. The data (points with error bars) are compared to the results of the overall fit (solid histogram). (b) $\mathcal{G}(w)|V_{cb}|$ distribution corrected for the reconstruction efficiency, with the fit result superimposed.

gion. Background components that peak in the m_{ES} signal region include cascade B meson decays, for which the lepton does not come directly from the B , and hadronic decays, and are subtracted using the corresponding MC predictions. The inclusive $\bar{B} \rightarrow X \ell^- \bar{\nu}_\ell$ yield is obtained from a maximum likelihood fit to the m_{ES} distribution of the B_{tag} candidates, as described in Ref. [21]. The fit yields $(198.9 \pm 1.6) \times 10^3$ events for the $B^- \rightarrow X \ell^- \bar{\nu}_\ell$ sample and $(116.3 \pm 1.0) \times 10^3$ events for the $\bar{B}^0 \rightarrow X \ell^- \bar{\nu}_\ell$ sample. The corresponding reconstruction efficiencies, including the B_{tag} reconstruction, are 0.39% and 0.25%, respectively.

Numerous sources of systematic uncertainty are investigated. The largest uncertainties are due to differences in the efficiency of the B_{tag} selection between the exclusive $\bar{B} \rightarrow D \ell^- \bar{\nu}_\ell$ and inclusive $\bar{B} \rightarrow X \ell^- \bar{\nu}_\ell$ decays

(a relative 1.5% systematic uncertainty on $|V_{cb}|$), the $\bar{B} \rightarrow D \ell^- \bar{\nu}_\ell$ fit procedure (1.3%), and the uncertainties on the branching fractions of the reconstructed D decay modes and $\bar{B} \rightarrow D^{**} \ell^- \bar{\nu}_\ell$ decays (1.1%). The uncertainties due to the detector simulation are established by varying, within bounds given by data control samples, the tracking efficiency of all charged tracks (0.7%), the calorimeter efficiency (0.9%), and the lepton identification efficiency (0.9%). We evaluate the systematic uncertainties associated with the MC simulation of various signal and background processes: photon conversion and π^0 Dalitz decay, B cascade decay contamination (0.8%), and flavor cross-feed (0.2%). The uncertainty arising from radiative corrections (0.1%) is studied by comparing the standard results with those obtained when PHOTOS is not used. We take 30% of the difference as a conservative systematic uncertainty. We vary the $\bar{B} \rightarrow D^* \ell^- \bar{\nu}_\ell$ form factors (0.4%) within their measured uncertainties [4] and use an HQET parameterization [22] to describe $\bar{B} \rightarrow D^{**} \ell^- \bar{\nu}_\ell$ decays (0.3%). We evaluate an uncertainty associated with the $\bar{B} \rightarrow X \ell^- \bar{\nu}_\ell$ fitting procedure (0.8%), and with the absolute branching fraction $\mathcal{B}(\bar{B} \rightarrow X \ell^- \bar{\nu}_\ell)$ used for the normalization (0.8%). The complete set of systematic uncertainties is given in Ref. [23].

From the fit to the combined $\bar{B} \rightarrow D \ell^- \bar{\nu}_\ell$ sample, we measure $\mathcal{G}(1)|V_{cb}| = (43.0 \pm 1.9 \pm 1.4) \times 10^{-3}$. Using an unquenched lattice calculation [11], corrected by a factor of 1.007 for QED effects, we obtain $|V_{cb}| = (39.8 \pm 1.8 \pm 1.3 \pm 0.9_{FF}) \times 10^{-3}$, where the third error is due to the theoretical uncertainty in $\mathcal{G}(1)$. As an alternative, we use a quenched lattice calculation based on the Step Scaling Method (SSM) [12], and obtain $|V_{cb}| = (41.6 \pm 1.8 \pm 1.4 \pm 0.7_{FF}) \times 10^{-3}$. The authors of [12] report the lattice determination of $\mathcal{G}(w)$ for finite momentum transfer. Although quenched, this new calculation allows the extraction of $|V_{cb}|$ with relatively small model dependence avoiding the large extrapolation to $w = 1$. For example, from a linear interpolation around $w = 1.2$, we obtain $|V_{cb}| = (41.4 \pm 1.3 \pm 1.4 \pm 1.0_{FF}) \times 10^{-3}$. We report our measurements of $\mathcal{G}(w)|V_{cb}|$ for $w > 1$ in Ref. [23].

The resulting value of $|V_{cb}|$ extrapolated to $w = 1$ is

largely independent of previous *BABAR* results [4] and significantly more precise than previous measurements from $\bar{B} \rightarrow D\ell^-\bar{\nu}_\ell$ decays. It is also consistent with the measurement obtained from $\bar{B} \rightarrow D^*\ell^-\bar{\nu}_\ell$ decays and with the inclusive determination of $|V_{cb}| = (41.6 \pm 0.6) \times 10^{-3}$ [5].

We are grateful for the excellent luminosity and machine conditions provided by our PEP-II colleagues, and for the substantial dedicated effort from the computing organizations that support *BABAR*. The collaborating institutions wish to thank SLAC for its support and kind hospitality. This work is supported by DOE and NSF (USA), NSERC (Canada), CEA and CNRS-IN2P3 (France), BMBF and DFG (Germany), INFN (Italy), FOM (The Netherlands), NFR (Norway), MIST (Russia), MEC (Spain), and STFC (United Kingdom). Individuals have received support from the Marie Curie EIF (European Union) and the A. P. Sloan Foundation.

Nucl. Phys. **B530**, 153 (1998).

- [15] B. Aubert *et al.* (*BABAR* Collaboration), Nucl. Instrum. Methods **A479**, 1 (2002).
- [16] D. Scora and N. Isgur, Phys. Rev. **D52**, 2783 (1995). See also N. Isgur *et al.*, Phys. Rev. **D39**, 799 (1989).
- [17] J. L. Goity and W. Roberts, Phys. Rev. **D51**, 3459 (1995).
- [18] E. Barberio and Z. Was, Comp. Phys. Commun. **79**, 291 (1994).
- [19] B. Aubert *et al.* (*BABAR* Collaboration), Phys. Rev. Lett. **92**, 071802 (2004).
- [20] R. J. Barlow and C. Beeston, Comput. Phys. Commun. **77**, 219 (1993).
- [21] B. Aubert *et al.* (*BABAR* Collaboration), Phys. Rev. Lett. **100**, 151802 (2008).
- [22] A. K. Leibovich, Z. Ligeti, I. W. Stewart and M. B. Wise, Phys. Rev. **D57**, 308 (1998).
- [23] See EPAPS Document No. *xxxxx*. For more information on EPAPS, see <http://www.aip.org/pubservs/epaps.html>.

* Deceased

† Now at Temple University, Philadelphia, Pennsylvania 19122, USA

‡ Also with Università di Perugia, Dipartimento di Fisica, Perugia, Italy

§ Also with Università di Roma La Sapienza, I-00185 Roma, Italy

¶ Now at University of South Alabama, Mobile, Alabama 36688, USA

** Also with Laboratoire de Physique Nucléaire et de Hautes Energies, IN2P3/CNRS, Université Pierre et Marie Curie-Paris6, Université Denis Diderot-Paris7, F-75252 Paris, France

†† Also with Università di Sassari, Sassari, Italy

- [1] M. Kobayashi and T. Maskawa, Prog. Theor. Phys. **49**, 652 (1973).
- [2] G. Buchalla *et al.*, Rev. Mod. Phys. **68**, 1125 (1996).
- [3] O. Buchmuller and H. Flacher, Phys. Rev. **D73**, 073008 (2006); C. Schwanda *et al.* (Belle Collaboration), Phys. Rev. **D78**, 032016 (2008).
- [4] B. Aubert *et al.* (*BABAR* Collaboration), Phys. Rev. **D79**, 012002 (2009) and references therein.
- [5] C. Amsler *et al.*, Phys. Lett. **B667**, 1 (2008).
- [6] K. Abe *et al.* (Belle Collaboration), Phys. Lett. **B526**, 258 (2002).
- [7] J. Bartele *et al.* (CLEO Collaboration), Phys. Rev. Lett. **82**, 3746 (1999).
- [8] D. Buskulic *et al.* (ALEPH Collaboration), Phys. Lett. **B395**, 373 (1997).
- [9] The charge conjugate state is always implied unless stated otherwise.
- [10] N. Isgur and M. B. Wise, Phys. Lett. **B237**, 527 (1990).
- [11] M. Okamoto *et al.*, Nucl. Phys. (Proc. Supp.) **140**, 461 (2005).
- [12] G.M. de Divitiis *et al.*, Phys. Lett. **B655**, 45 (2007).
- [13] I. Caprini and M. Neubert, Phys. Lett. **B380**, 376 (1996), and C. G. Boyd, B. Grinstein, R. F. Lebed, Phys. Rev. **D56**, 6895 (1997).
- [14] I. Caprini, L. Lellouch, M. Neubert,

Electronic Physics Auxiliary Publication Service (EPAPS)

This is an EPAPS attachment to B. Aubert *et al.* (BABAR Collaboration), BABAR-PUB-09/009, SLAC-PUB-13580, submitted to Phys. Rev. Lett. For more information on EPAPS, see <http://www.aip.org/pubservs/epaps.html>.

TABLE II: Systematic uncertainties in the measurement of $\mathcal{G}(1)|V_{cb}|$, ρ^2 and the branching fraction for $\bar{B} \rightarrow D\ell^-\bar{\nu}_\ell$ decays. We report the relative error (in %) for $\mathcal{G}(1)|V_{cb}|$ and branching fraction, and the absolute error on ρ^2 .

	Systematic uncertainty on $ V_{cb} $, ρ^2 and BF								
	$D^0\ell^-\bar{\nu}_\ell$			$D^+\ell^-\bar{\nu}_\ell$			$D\ell^-\bar{\nu}_\ell$		
	$ V_{cb} (\%)$	ρ^2	BF (%)	$ V_{cb} (\%)$	ρ^2	BF (%)	$ V_{cb} (\%)$	ρ^2	BF (%)
Tracking efficiency	0.5	0.008	0.7	1.1	0.003	1.4	0.7	0.004	1.0
Neutral reconstruction	1.0	0.003	1.2	0.8	0.006	0.9	0.9	0.004	1.2
Lepton ID	1.0	0.009	1.0	0.9	0.009	0.8	0.9	0.009	0.9
Final State Radiation	0.1	0.005	0.2	0.1	0.005	0.2	0.1	0.005	0.2
Cascade $\bar{B} \rightarrow X \rightarrow \ell^-$ decay background	0.6	-	1.2	1.0	-	2.0	0.8	-	1.5
$B^0 - B^\pm$ cross-feed	0.2	0.003	0.2	0.2	0.003	0.2	0.2	0.003	0.2
$\bar{B} \rightarrow D^*\ell^-\bar{\nu}_\ell$ form factors	0.6	0.008	0.5	0.2	0.003	0.2	0.4	0.006	0.3
$\bar{B} \rightarrow D^{**}\ell^-\bar{\nu}_\ell$ form factors	0.2	0.007	0.2	0.3	0.006	0.2	0.3	0.007	0.1
D branching fractions	1.0	-	2.0	1.4	-	2.7	1.1	-	2.2
$\mathcal{B}(\bar{B} \rightarrow D^{**}\ell^-\bar{\nu}_\ell)$	1.2	0.023	0.6	1.0	0.011	0.9	1.1	0.019	0.6
$\mathcal{B}(\bar{B} \rightarrow X\ell^-\bar{\nu}_\ell)$	0.9	-	1.9	0.9	-	1.9	0.8	-	1.7
B_{tag} selection	1.1	0.021	0.6	1.8	0.036	0.8	1.5	0.028	0.8
$\bar{B} \rightarrow X\ell^-\bar{\nu}_\ell$ fit	0.7	-	1.4	1.1	-	2.2	0.8	-	1.7
$\bar{B} \rightarrow D\ell^-\bar{\nu}_\ell$ fit	1.3	0.018	1.1	1.1	0.027	0.6	1.3	0.020	0.8
B meson lifetime	-	-	0.7	-	-	0.6	-	-	0.6
Total systematic error	3.1	0.04	4.1	3.6	0.05	5.0	3.3	0.04	4.3

TABLE III: Fit results for $|V_{cb}|\mathcal{G}(w)$ extracted at different value of w . In order to reduce any fit model dependence, we fit the data interpolating few bins around w . In particular we use 4 bins between $w = 1.00$ and $w = 1.24$ to extract $|V_{cb}|\mathcal{G}(w)$ at $w = 1.03, 1.05$ and 1.10 , and 4 bins between $w = 1.06$ and $w = 1.30$ to extract $|V_{cb}|\mathcal{G}(w = 1.20)$. The statistical correlation between the measurement at $w = 1.20$ and the others is $\rho_{\text{corr}} = 0.57$, instead the systematic uncertainties can be assumed correlated at 100%. In the last column we report the results for $|V_{cb}|$ obtained using the results for the $\mathcal{G}(w)$ computed in G.M. de Divitiis *et al.*, Phys. Lett. B**655**, 45 (2007).

w	$ V_{cb} \cdot \mathcal{G}(w) \cdot 10^3$	$\mathcal{G}(w)$	$ V_{cb} \cdot 10^3$
1.03	$40.9 \pm 5.7 \pm 1.3$	1.001 ± 0.019	$40.9 \pm 5.7 \pm 1.3 \pm 0.8$
1.05	$40.2 \pm 5.0 \pm 1.3$	0.987 ± 0.015	$40.7 \pm 5.1 \pm 1.3 \pm 0.6$
1.10	$38.3 \pm 3.3 \pm 1.3$	0.943 ± 0.011	$40.6 \pm 3.5 \pm 1.4 \pm 0.5$
1.20	$35.3 \pm 1.1 \pm 1.2$	0.853 ± 0.021	$41.4 \pm 1.3 \pm 1.4 \pm 1.0$